Drug Design, Development and Therapy

Dovepress
open access to scientific and medical research

Open Access Full Text Article

ORIGINAL RESEARCH

Sichen Formula Ameliorates Lipopolysaccharide-Induced Acute Lung Injury via Blocking the TLR4 Signaling Pathways

Li-Shan Yan[1,*], Shuang Cui[1,*], Brian Chi-Yan Cheng[2], Xing-Bin Yin[1], Yi-Wei Wang[1], Xin-Yu Qiu[1], Ci-Ren Nima[3], Yi Zhang[1], Shuo-Feng Zhang[1]

[1]School of Chinese Materia Medica, Beijing University of Chinese Medicine, Beijing, People's Republic of China; [2]College of Professional and Continuing Education, Hong Kong Polytechnic University, Hong Kong, People's Republic of China; [3]Tibetan Traditional Medical College, Lhasa, Tibet, People's Republic of China

*These authors contributed equally to this work

Correspondence: Shuo-Feng Zhang; Yi Zhang, School of Chinese Materia Medica, Beijing University of Chinese Medicine, No. 11, Bei San Huan Dong Lu, Chaoyang District, Beijing, 100029, People's Republic of China, Tel/Fax +86-10-53912122, Email shuofengzhang@sina.com; yizhang714@163.com

Purpose: Sichen (SC) formula is a classic prescription of Tibetan medicine. Due to its potential anti-inflammatory effect, the SC formula has been clinically used to treat respiratory diseases for many years in the Chinese Tibet region. The present study aimed to investigate the anti-inflammatory effect of SC and explore the underlying mechanisms.

Methods: SC formula was characterized by HPLC analysis. The acute lung injury (ALI) mouse model was induced by direct intratracheal lipopolysaccharide (LPS) instillation, and bronchoalveolar lavage fluid (BALF) and lung tissues were collected. Meanwhile, RAW264.7 macrophages were stimulated by LPS. The contents of inflammatory mediators in the culture medium were determined by ELISA. Protein levels were determined by immunohistochemical staining or Western blotting. Nuclear localization of NF-κB, AP-1, and IRF3 was performed using immunofluorescence and Western blotting.

Results: In the LPS-induced ALI mouse model, SC treatment suppressed the secretion of inflammatory mediators (TNF-α, IL-6, IL-1β, MCP-1, MIP-1α, and RANTES) in BALF. SC treatment hindered the recruitment of macrophages. SC treatment also inhibited the expression of CD68, p-p65, and TLR4 in the lung tissue. In the LPS-exposed RAW264.7 cells, the cell viability was not changed up to 400 μg/mL of SC. SC concentration-dependently suppressed the production of nitric oxide, prostaglandin E2, TNF-α, IL-6, MCP-1, MIP-1α, and RANTES in LPS-challenged RAW264.7 cells. The expression levels of iNOS, COX-2, p-p38, p-JNK, p-ERK, p-TBK1, p-IKKα/β, p-IκB, p-p65, p-c-Jun, and p-IRF3 were decreased after SC treatment. Moreover, the nuclear translocation of p65, c-Jun, and IRF3 was also blocked by SC treatment.

Conclusion: SC treatment inhibited the inflammatory responses in LPS-induced ALI mouse model/RAW264.7 macrophages. The underlying mechanism of this action may be closely associated with the suppression of TLR4 signaling pathways. These research findings provide further pharmacological justifications for the medicinal use of SC in the management of respiratory diseases.

Keywords: Sichen formula, acute lung injury, RAW264.7 macrophages, lipopolysaccharide, TLR4 signaling pathways

Introduction

Acute lung injury (ALI) and its most severe form, acute respiratory distress syndrome (ARDS), manifest as severe lung inflammation characterized by endothelial and epithelial injury, deposition of platelets, and leukocyte aggregation.[1] ALI, which often results in fulminant respiratory failure and death, has multiple etiologies, including sepsis, pneumonia, aspiration, and trauma.[2,3] ALI/ARDS is the dominant cause of morbidity in intensive care units, along with hospital mortality of 40%.[4] The overall management of ALI/ARDS focuses on supportive care and pharmacological therapy. Mechanical ventilation is an essential part of the care since no proven pharmacological treatment for ALI/ARDS is currently available to maintain adequate oxygenation and carbon dioxide elimination.[5] Corticosteroid treatment is widely

Received: 1 May 2022
Accepted: 21 December 2022
Published: 2 February 2023

used for improving gaseous exchange and hemodynamic stability in the management of ALI. However, prolonged corticosteroid therapy could cause severe adverse effects, including hyperglycemia and infections.[6] Therefore, safety and effective agents are urgently needed for halting or reversing the progression of ALI.

Participating in the innate mechanism for clearing respirable particles and microbial organisms, macrophages also play an essential role in the development and progression of many respiratory diseases, including ALI.[7] Macrophages could detect endogenous danger signals in the lung interstitium and alveoli, such as lipopolysaccharide (LPS), a component of Gram-negative bacteria, which binds to the pattern-recognition receptor, Toll-like receptor 4 (TLR4).[8] This binding initiates the intracellular signaling cascades, promoting phosphorylation of downstream effectors, such as inhibitor of nuclear factor-κB (IκB) and IκBα kinase (IKK) complex, which, in turn, activates and accelerates the nuclear translocation of NF-κB.[9] Furthermore, other key protein kinases, including c-Jun N-terminal kinase (JNK), mitogen-activated protein kinase (MAPK) p38, and extracellular signal-regulated kinase (ERK), are activated, causing subsequent phosphorylation and nuclear translocation of activator protein 1 (AP-1).[10] Additionally, activation of TLR4 induces the phosphorylation of TANK-binding kinase 1 (TBK1), an IKK-related kinase that phosphorylates and activates downstream targets, such as interferon regulatory factor 3 (IRF3), triggering its dimerization and nuclear translocation. Once these transcription factors translocate into the nucleus, the production of various cytokines and chemokines is substantially enhanced, thereby exacerbating the degree of lung injury.[11] Therefore, suppressing TLR4 signaling emerges as an attractive therapeutic strategy for limiting inflammation in the management of ALI.

Sichen (SC) formula, a classic prescription based on Tibetan medical theory, consists of four herbal medicines, including *Radix Phlomii* (dried tuberous root of *Phlomoides younghushandii* [Mukerjee] [family: Lamiaceae]), *Rhizoma Bergeniae* (dried rhizome of *Bergenia purpurascens* [Hook.f.et Thoms.] Engl. [family: Saxifragaceae]), *Herba Artemisiae scoparae* (dried overground part of *Artemisia scoparia* Waldst. and Kit. [family: Asteraceae]), and *Radix Glycyrrhizae* (dried root and rhizome of *Glycyrrhiza uralensis* Fisch., *G. inflata* Bat., or *G. glabra* L. [family: Fabaceae]) at the ratio of 1.5:1:2:2. It has been reported that SC formula has potential heat-clearing, desiccating, cough-relieving, and phlegm-eliminating properties.[12] SC has been used clinically to treat different types of respiratory diseases, such as respiratory infections, chronic bronchitis, and asthma, for many years.[13,14] However, scant reports have been issued on the anti-ALI effect of SC, and the underlying mechanism of this action is still unknown. Therefore, in this study, we established an LPS-induced ALI mouse model to investigate the anti-inflammatory effects of SC regarding ALI. We also used LPS-stimulated RAW264.7 macrophages to explore the underlying molecular mechanism of this action.

Materials and Methods

Materials

Modified Griess reagent, 3-[4,5-dimethylthiazol-2-yl]-2,5-diphenyl tetrazolium bromide (MTT), Wright stain solution, and LPS (*Escherichia coli* O55:B5) were purchased from Sigma Chemical Co. (St. Louis, MO, USA). Penicillin–streptomycin solution was obtained from Caisson labs (Smithfield, UT, USA). Fetal bovine serum (FBS) was bought from Biological Industries Co. (Beth-Haemek, Israel). Dexamethasone was obtained from Tianjin Lisheng Pharmaceutical Co., Ltd. Dulbecco's Modified Eagle Medium (DMEM) was acquired from Corning Cellgro (Manassas, VA, USA). Tumor necrosis factor α (TNF-α, 88-7324-22), interleukin-6 (IL-6, 88-7064-22), IL-1β (88-7013-22), macrophage inflammatory protein 1α (MIP-1α, 88-56013-22), monocyte chemoattractant protein 1 (MCP-1, 88-7391-22), and regulated upon activation normal T cell expressed and secreted factor (RANTES, KMC1031) enzyme-linked immunosorbent assay (ELISA) kits were purchased from Thermo Fisher Scientific (San Diego, CA). Prostaglandin E2 (PGE2, ADI-900-001) ELISA kit was provided by Enzo Life Sciences (Exeter, UK). Anti-CD68 (cat no. sc-20060), TLR4 (cat no. sc-293072), GAPDH (cat no. sc-365062) and phospho-NF-κB p65 (Ser536, cat no.sc-136548, for immunohistochemical staining) monoclonal antibodies were supplied by Santa Cruz Biotechnology (Santa Cruz, CA, USA). Anti-IKKβ (cat no. 15649-1-AP) and Sp1 (cat no. 21962-1-AP) antibodies were from Proteintech (Rosemont, USA). Antibody against IRF3 (cat no. ab68481), anti-inducible nitric oxide synthase (iNOS, cat no. ab3523), anti-mouse immunoglobulin (Ig)G, and HRP-conjugated secondary antibody (cat no. ab6789) were purchased from Abcam (Cambridge, UK). Antibody against phospho-IRF3 (Ser 396, cat no. PAB31634) was provided by ABNOVA

(Taiwan, China). Antibodies against NF-κB p65 (cat no. 8242), phospho-NF-κB p65 (Ser536, cat no. 3033, for Western blot), c-Jun (cat no. 9165), phospho-c-Jun (Ser73, cat no. 9164), cyclooxygenase-2 (COX-2, cat no. 12282), IκBα (cat no. 4814), phospho-IκBα (Ser32, cat no. 2859), phospho-IKKα/β (Ser176/177, cat no. 2697), ERK (cat no. 4697), phospho-ERK (Thr202/Tyr204, cat no. 4370), JNK (cat no. 9252), phospho-JNK (Thr183/Tyr185, cat no. 4668), p38 MAPK (cat no. 8690), phospho-p38 (Thr180/Tyr182, cat no. 4511), TBK1 (cat no. 3013), phospho-TBK1 (Ser172, cat no. 5483), β-actin (cat no. 4970), anti-rabbit IgG HRP linked antibody (cat no. 7074), and Alexa Fluor 488-conjugated secondary antibody (cat no. 4412) were bought from Cell Signaling Technology (Boston, MA, USA). Stripping buffer (SW3020) was bought from Solarbio (Beijing, China). The reference standards, including chlorogenic acid (LOT #: 110753-201817), bergenin (LOT #: 111532-201604), and ammonium glycyrrhizate (LOT #: 110731-202021) were supplied by the National Institutes for Food and Drug Control.

Preparation of SC

Radix Phlomii, Rhizoma Bergeniae, Herba Artemisiae scoparae, and *Radix Glycyrrhizae* were provided by the Tibetan Traditional Medical College. All of them were authenticated by Prof. Ci-Ren Nima. Voucher specimens have been deposited at the Department of Pharmacology, School of Chinese Medicine, Beijing University of Chinese Medicine. Air-dried crude drugs composing SC formula (*Radix Glycyrrhizae: Herba Artemisiae scoparae: Radix Phlomii: Rhizoma Bergeniae*: = 4:4:3:2, 6500 g in total) were extracted three times by refluxing with eight times amount of water for 1.5 h each time. The combined water extract was concentrated by reducing pressure at 90°C and dried by vacuum at 70°C. The SC powder was then obtained.

Characterization of SC by High-Performance Liquid Chromatography (HPLC)

The porphyrized SC powder was sonicated with 50% methanol for 30 min and filtered to characterize SC. The contents of bergenin, chlorogenic acid, and ammonium glycyrrhizate in the filtrate were determined by a chromatographic analysis performed on a Shimadzu LC-20A HPLC system (Shimadzu, Japan). The separation was performed on an Acclaim™ 120 C18 column (4.6 mm × 250 mm, 5 μm, Thermo Fisher Scientific, USA) at 20°C. The mobile phase consisted of solvent A (acetonitrile) and solvent B (0.1% phosphoric acid water) with the gradient program as follows: 0−16 min, 4% to 8% A; 16−30 min, 8% to 9% A; 30−50 min, 9% to 16% A; 50−70 min, 16% to 17% A; 70−73 min, 17% to 20% A; 73−93 min, 20% to 28% A; 93−105 min, 28% to 43% A; 105−120 min, 43% to 50% A. The flow rate was maintained at 0.8 mL/min, and the chromatograms were monitored with the PDA detector at a wavelength of 254 nm. Each sample of 10 μL was injected for analysis.

Molecular Docking

The crystal structure of TLR4 came from the Protein Data Bank (PDB code: 2Z66). The ligands and water molecules were removed from the crystal structure via Pymol (https://pymol.org/2/). The structure of bergenin, chlorogenic acid, and ammonium glycyrrhizate (ammonium removed) was obtained from PubChem database (https://pubchem.ncbi.nlm.nih.gov/) and hydrogen atoms were added by using AutoDock Vina software. The rigid target-site docking procedures were performed using AutoDock vina software with a genetic algorithm.[15] Hydrogen bonds and bond lengthanalysis and visualization were performed using Pymol.

Mouse Model of ALI

Male BALB/c mice weighing 18–22 g were obtained from SPF Biotechnology Co., Ltd (Beijing, People's Republic of China) and maintained in the animal facility at the Department of Pharmacology, School of Chinese Materia Medica, Beijing University of Chinese Medicine. All experimental procedures followed the National Institutes of Health Guide for the Care and Use of Laboratory Animals and were approved by the University Committee on Research Practice at the Beijing University of Chinese Medicine. Mice were housed with a 12 h light/dark cycle at 20–22°C with a relative humidity of 50–55% and provided with free access to water and food. Mice were divided into six groups of 10 mice: (1) control mice, (2) model mice, (3) mice receiving SC at 2.7 g/kg/d (0.5-fold human equivalent dose) intragastrically, (4) mice receiving SC at 5.4 g/kg/d (human equivalent dose) intragastrically, (5) mice receiving SC at 10.8 g/kg/d (2-fold

human equivalent dose) intragastrically, (6) and mice receiving dexamethasone at 1.8 mg/kg/d intragastrically. The mice in the control and model groups were given PBS. The mice in other groups were given corresponding drugs intragastrically for five consecutive days. Eighteen hours after the last gavage, mice were anesthetized with 50 mg/kg of sodium pentobarbital and LPS (125 μg/mouse) dissolved in PBS, or PBS alone was administered intratracheally between 3 and 6 PM. Time between 9 and 12 AM next day (18 h from intratracheally administration of LPS or PBS),[16] bronchoalveolar lavage was performed with an intratracheal injection of 0.3 mL PBS solution into the right lung following gentle aspiration three times. The bronchoalveolar lavage fluid (BALF) was centrifuged for 8 min at 2000 ×*g* and 4°C. The cell pellet was collected and resuspended in PBS, and the number of cells in each sample was counted using a hemocytometer. The remaining cell suspension was thinly spread over a glass slide, air dried, and stained with the Wright stain solution according to the manufacturer's instructions to determine the differential immune cells. The BALF supernatants were then stored at −80°C until use, and the left lung tissue samples were dissected for subsequent experiments.

Hematoxylin and Eosin (HE) Staining

A small block of the lung tissue was dissected and fixed in 10% neutral buffered formalin and then embedded in paraffin. Subsequently, the paraffin block was cut into 5-μM slices, which were stained with hematoxylin and eosin, according to the manufacturer's protocol. Representative areas were photographed under the viewing of a Nikon Eclipse Ts2R microscope (Nikon, Tokyo, Japan) at 200× magnification. Each lung tissue slice was scored by a blind observer according to the presence of (1) goblet cell hyperplasia, (2) hemorrhage, and (3) infiltration or aggregation of inflammatory cells in the bronchial lumen and bronchoalveolar tissue. Each item was graded from 0 to 4 (absent, minimal, mild, moderate, or severe injury), and all scores were added up to obtain a total pathological score.[17] Ten lung tissue samples for each group were used.

Immunohistochemical Staining of CD68, TLR4, and p-p65

The paraffin sections of lung tissue were deparaffinized and rehydrated, followed by antigen retrieval with citric acid for 45 min. After blocking with hydrogen peroxide solution for 10 min, the slides were washed with PBS three times and incubated with primary antibodies against CD68, TLR4, or p-p65 for 2 h at room temperature. The slides were then washed with PBS three times and incubated with biotinylated goat anti-mouse IgG secondary antibody (ZSGB-BIO, Beijing, China) for 20 min. Followed by 3, 3′-diaminobenzidine (DAB) chromogenic reaction, the sections were counterstained with hematoxylin stain, dehydrated, and mounted. Images were taken using a Nikon Eclipse Ts2R microscope (Nikon, Tokyo, Japan). For quantitative analysis of CD68, TLR4, and p-p65 expression, the positive staining area was measured via Image-Pro Plus 5.1 software (Media Cybernetics, Rockville, MD, USA). Three images of each lung tissue slice were analyzed. Ten lung tissue samples for each group were used.

Cell Culture

The RAW264.7 mouse macrophage cell line was kindly gifted by Prof. Zhi-Xiang Zhu (Beijing University of Chinese Medicine, China). Cells were maintained in DMEM supplemented with 10% fetal bovine serum, 100 U/mL penicillin, and 100 U/mL streptomycin in a CO_2 incubator (under a humidified atmosphere of 5% CO_2 and 95% air) at 37°C.

Cell Viability Assay

Cells were seeded (6×10^3 cells/well) and cultured in 96-well plates, followed by treatment with LPS (1 μg/mL) and various concentrations of SC (6.25–400 μg/mL) for 24 h at 37°C. Ten μL of the MTT solution (5 mg/mL) was added to each well and incubated for about 4 h at 37°C. Subsequently, the supernatant was removed, and the remaining formazan crystals were dissolved in 100 μL DMSO in each well. The absorbance at 570 nm was detected using a microplate spectrophotometer (BMG SPECTROstar Nano, Germany). The value of cell viability in the control group was set at 100%. Six replicate wells were used.

Determination of Inflammatory Mediators

The contents of cytokines and chemokines in the culture medium and BALF were quantified by ELISA kits. Briefly, cells were seeded into 24-well plates (2×10^5 cells/well) for 24h. The cells were then treated with SC (50–400 μg/mL) for 1h and then treated with or without LPS (1 μg/mL) for 24h. The cell-free supernatants were collected for the detection of the levels of PGE2, IL-6, TNF-α, MCP-1, MIP-1α, and RANTES using ELISA kits according to the manufacturer's instructions. The contents of nitric oxide were determined by Griess reagent. Four replicates for cell-free supernatants were used. For BALF, IL-6, IL-1β, TNF-α, MCP-1, MIP-1α, and RANTES were detected following the manufacturer's instructions. A total of 7–8 BALF samples for each group were used.

Western Blotting

The targeted protein levels of lung tissue and cell lysates were assessed by Western blotting analysis as described previously.[18] Briefly, RAW264.7 cells were treated with SC at 200 and 400 μg/mL. LPS (1 μg/mL) was then added to the culture medium after SC pretreatment, and the cells were incubated at 37°C for 30 min. The collected cells and lung tissue were lysed with RIPA buffer (Beyotime Biotechnology, Beijing, China). The nuclear/cytoplasmic fractions were isolated using a nuclear extraction kit (Solarbio, Beijing, China) following the manufacturer's instructions. An aliquot of 40 μg of the supernatant protein from each sample was heated with 4 × sodium dodecyl sulfate sample buffer at 95°C for 8 min and then subjected to 10% SDS-PAGE and electro-transferred onto a polyvinylidene fluoride membrane. The membranes were blocked by 5% non-fat milk dissolved in TBST for 1 h at room temperature. The target proteins were detected using the indicated primary antibodies overnight at 4°C. The membranes were then incubated with anti-mouse or anti-rabbit secondary antibody for 1h and then washed by TBST for three times. The specific immunoreactive bands were detected using an enhanced chemiluminescence detection kit (Tanon, Shanghai, China) and exposed to the Tanon 5200 Chemiluminescent Imaging System. The bands were quantified using the ImageJ software (National Institutes of Health, Bethesda, MD, USA). The protein levels were normalized to the matching densitometric value of the internal control (β-actin/GAPDH/Sp1). Six lung tissue samples and five cell samples for each group were used.

Immunofluorescence Staining

Immunofluorescence staining was performed to detect the nuclear translocation of transcriptional factors, including NF-κB, AP-1, and IRF3, as our previously described.[19] Briefly, the cells (1×10^4) were seeded into a chamber slide for 24 h. Then, the cells were treated with SC (200 and 400 μg/mL) for 1 h. After LPS (1 μg/mL) treatment for 30 min, the cells were fixed with formaldehyde in PBS (w:v, 4%) for 15 min. Subsequently, cells were permeabilized by Triton X-100 (0.25%) for 30 min at 37°C, and then blocked for 1 h with BSA (2%) and incubated with indicated primary antibodies overnight at 4°C. The cells were incubated with fluorescence-labeled goat anti-rabbit secondary antibody at room temperature for 1 h, and washed by PBST for three times. The nucleus was stained with 4′,6-diamidino-2-phenylindole (DAPI, YESEN, Shanghai, China). The slides were mounted by anti-fluorescence quenchers and then photographed under an A1R confocal microscope (Nikon, Japan). For fluorescence intensity quantification, 50 cells were analyzed in each group by ImageJ software as following: images were split into two channels and the nuclei were selected as regions of interest (ROIs). By the ROI Manager, the mean intensity of green fluorescence in the nuclear area was then measured.

Statistical Analysis

All values were expressed as the mean ± standard error of the mean (SEM). Data were analyzed using GraphPad Prism (version 9.0.0) statistical analysis program as follows: Shapiro–Wilk test (for $n > 5$) or QQ plot (for $n \leq 5$) was used to assess data normality. For data that passed normality test and F-test, ordinary one-way ANOVA was performed to compare statistical significance. For data that passed normality test but not F-test, Brown-Forsythe and Welch ANOVA tests were used. For non-normal distribution data, Kruskal–Wallis test was performed. A difference was considered to be significant when $p < 0.05$.

Results

Characterization of Sichen Formula

Three representative bioactive components, including bergenin, chlorogenic acid, and ammonium glycyrrhizate, which have been identified in *Rhizoma Bergeniae, Herba Artemisiae scoparae*, and *Radix Glycyrrhizae*, respectively,[20–22] were determined in SC by HPLC to control the quality of the prepared SC (Figure 1A–D). The mean contents of bergenin, chlorogenic acid, and ammonium glycyrrhizate occurring in SC were 36.8, 14.34, and 22.46 mg/g, respectively. Figure 1E shows that bergenin, chlorogenic acid, and ammonium glycyrrhizate directly interact with TLR4, with the binding energy of −4.46, −2.87 and −3.62 kcal/mol, respectively. Five residues (GLN-436, HIS-566, ASP-596, SER-589 and LEU-56) are involved in the hydrogen bond interactions with bergenin. Chlorogenic acid is found able to form hydrogen bonds with SER-39, LYS-62, GLN562 and GLU536. Moreover,

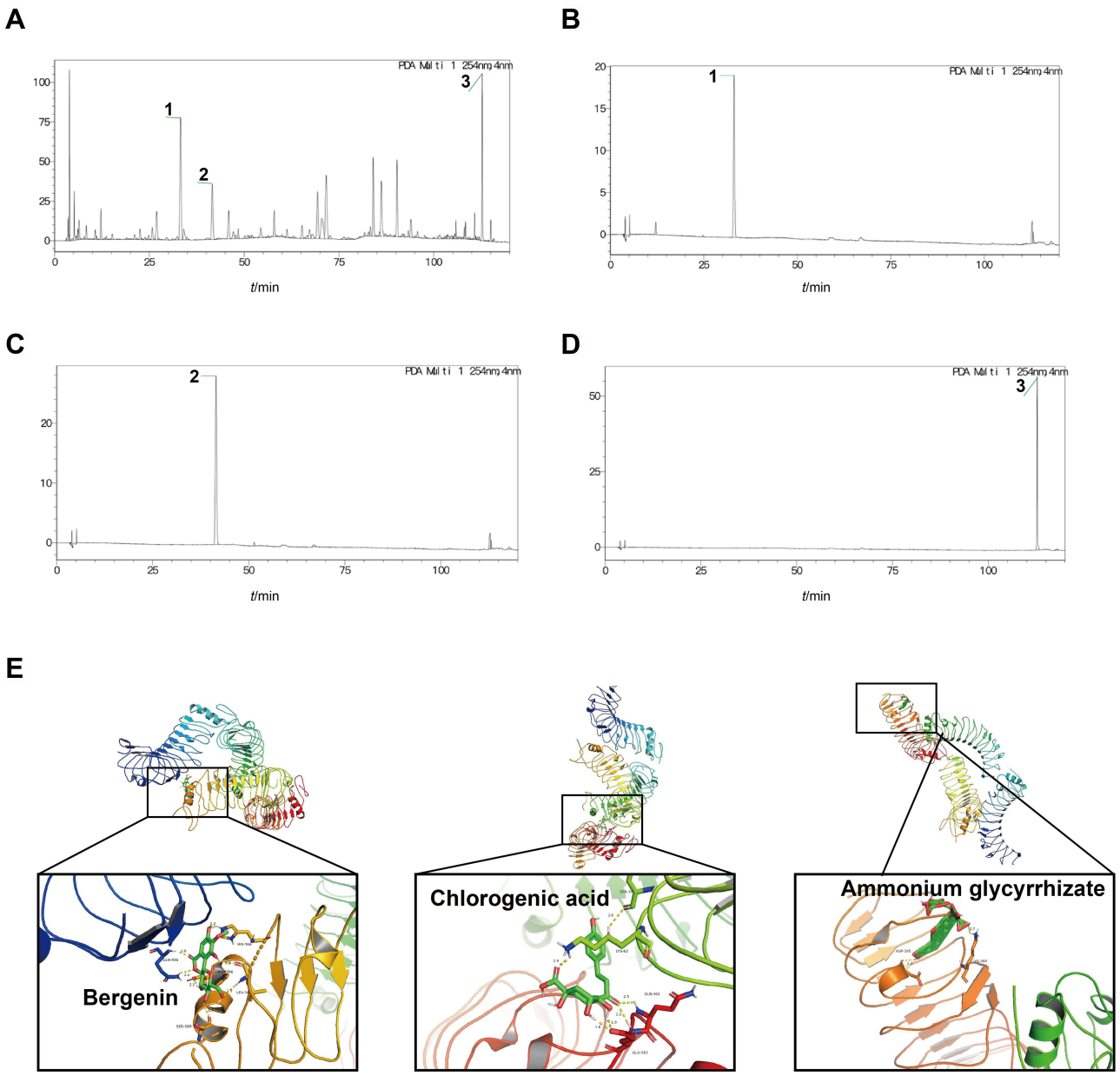

Figure 1 The HPLC chromatograms of bergenin, chlorogenic acid and ammonium glycyrrhizate in SC and their binding mode with TLR4. HPLC chromatogram of SC dissolved in 50% methanol (**A**), bergenin (**B**), chlorogenic acid (**C**) and ammonium glycyrrhizate (**D**) dissolved in 50% methanol. Peaks 1, 2, and 3 represent bergenin, chlorogenic acid and ammonium glycyrrhizate, respectively. (**E**) Molecular docking of bergenin, chlorogenic acid and ammonium glycyrrhizate (ammonium removed) with the crystal structure of TLR4 (PDB code: 2Z66) was modeled using AutoDock vina software and visualized via Pymol. Yellow dashed lines denote hydrogen bonds.

ASP-395 and LYS-388 form two hydrogen bonding contacts with ammonium glycyrrhizate. These findings suggest that SC may have potential to interact with TLR4, thus inhibiting TLR4-mediated inflammatory responses.

SC Treatment Ameliorated Lung Injury and LPS-Induced Inflammation in Mice

Next, we employed an LPS-induced ALI mouse model to evaluate the potential effects of SC on ALI. Histological analysis revealed that LPS administration triggered inflammatory cell infiltration and thickening of the alveolar wall and disrupted tight junctions of the alveolar epithelium. Pretreatment of mice with SC markedly inhibited the pathological changes caused by LPS, which was further supported by the reduction of pathological scores (Figure 2A). Moreover, the number of total immune cells was markedly increased after LPS treatment, and LPS exposure substantially promoted the recruitment of macrophages and neutrophil granulocytes to the bronchoalveolar region and increased these inflammatory cells in BALF. SC treatment at 10.8 g/kg reduced the influx of macrophages- caused by LPS (Figure 2B). Consistently, immunohistochemical staining of lung tissues from LPS-exposed mice showed the elevation of CD68-positive area compared with the control group. However, SC could reduce CD68-positive area value in lung tissue after LPS treatment, suggesting the alleviation of macrophage infiltration by SC treatment (Figure 2C). Furthermore, Figure 2D shows that SC treatment significantly decreased LPS-induced overproduction of pro-inflammatory cytokines (TNF-α, IL-1β, and IL-6) and chemokines (MCP-1, RANTES, and MIP-1α) in BALF. SC treatment also decreased the expression levels of TLR4 and p-p65 in lung tissue from LPS-treated mice (Figure 3), showing that SC has the potential to suppress the TLR4 signaling pathway.

SC Treatment Inhibited the Production of Pro-Inflammatory Mediators in LPS-Stimulated RAW264.7 Cells

The above-described findings implied that SC could alleviate macrophage-mediated lung inflammatory responses. We then investigated the anti-inflammatory effect of SC in LPS-activated RAW264.7 macrophages. As indicated by the MTT assay, no significant cytotoxic effect on cell viability was observed in RAW264.7 macrophages treated with SC at concentrations of up to 400 μg/mL (Figure 4A). Thus, we chose 50–400 μg/mL of SC for our next experiments. The secretion of NO and PGE2 was significantly elevated after LPS challenge, and SC treatment suppressed the production of these two inflammatory mediators in a concentration-dependent manner (Figure 4B and Figure 4C). The elevation of the essential enzymes responsible for NO and PGE2 synthesis induced by LPS stimulation, including iNOS and COX-2, was markedly decreased by SC treatment (Figure 4D). Moreover, SC treatment markedly decreased the release of IL-6 and chemokines (MCP-1, MIP-1α, and RANTES) in LPS-stimulated RAW264.7 macrophages. SC treatment suppressed the production of TNF-α caused by LPS stimulation, but there was no statistical significance compared to only LPS challenged cells (Figure 4E).

SC Treatment Suppressed the TLR4 Signaling Pathways in LPS Stimulated-RAW264.7 Cells

We then explored the inhibitory effect of SC on the TLR4 signaling pathways, which play essential roles in mediating the transcription of pro-inflammatory mediators,[23] to further investigate the underlying mechanism of the anti-inflammatory action of SC. Figure 5 reveals that the phosphorylation of p65, c-Jun, and IRF3 was significantly increased after LPS stimulation, and SC treatment decreased the expression of phosphorylated p65, c-Jun, and IRF3 in a concentration-dependent manner. Moreover, the stimulation of RAW264.7 macrophages with LPS resulted in the activation of MAPKs, including ERK, p38, and JNK, as evidenced by the elevation of phosphorylated proteins. SC treatment effectively inhibited the phosphorylation of ERK, p38, and JNK. Additionally, the exposure of RAW264.7 cells to LPS caused marked elevation of the phosphorylation of IκBα, IKKα/β, and TBK1, which are the required upstream events of NF-κB and IRF3 activation, whereas these effects were significantly abolished by SC treatment.

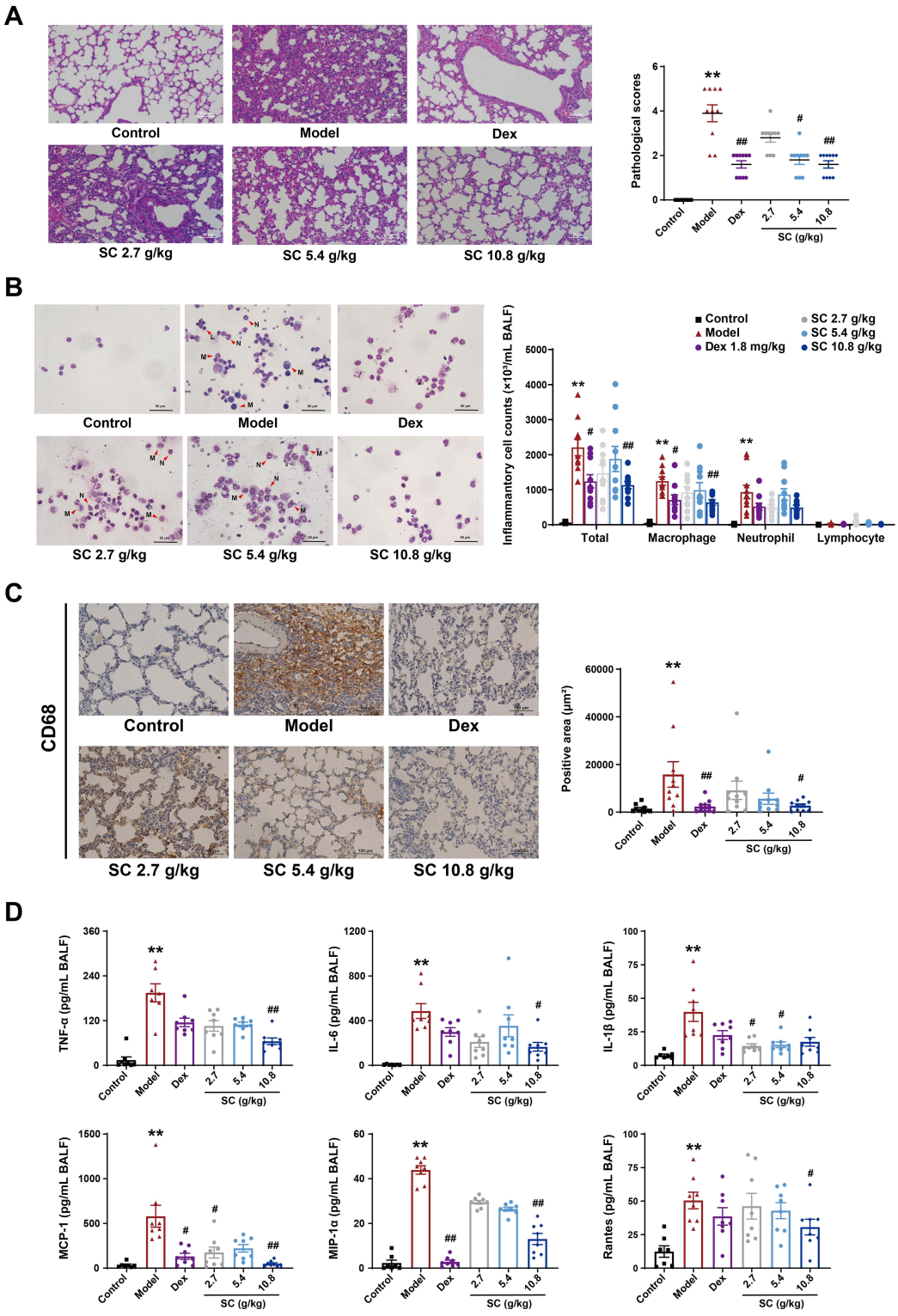

Figure 2 Effects of SC treatment on the respiratory inflammatory response in LPS-induced ALI mice. BALB/c mice received 5-day pretreatment of different doses of SC (2.7, 5.4 or 10.8 g/kg) or dexamethasone (1.8 mg/kg) and then intratracheally challenged with LPS (125 μg/mouse) for 18 hours. (**A**) Representative images of HE-stained lung sections. Morphology was examined using light microscopy and pathological scores were assessed (right panel, n=10/group, Kruskal–Wallis tests with Dunn's multiple comparisons as post hoc test). (**B**) Representative images of inflammatory cells from BALF with Wright staining. Total cell counts in BALF were determined by hematocytometer (n=10/group, Brown-Forsythe and Welch ANOVA tests with Dunnett's T3 multiple comparisons test). The number of macrophages, neutrophils and lymphocytes was analyzed under light microscopy (magnification 400×, n=10/group, Brown-Forsythe and Welch ANOVA tests for macrophage, Kruskal–Wallis tests for neutrophil and lymphocyte). Red arrowheads denote macrophages (M), neutrophils (N) and lymphocytes (L). (**C**) Immunohistochemical staining for CD68 and quantification of CD68-stained area in lung tissues (n=10/group, Kruskal–Wallis tests with Dunn's multiple comparisons as post hoc test). (**D**) Levels of TNF-α, IL-6, IL-1β, MCP-1, Rantes and MIP-1α in BALF were measured by ELISA (n=7–8/group, Kruskal–Wallis tests for TNF-α, IL-6, IL-1β, MCP-1 and MIP-1α, one-way ANOVA followed by Fisher's LSD for Rantes). Data are presented as the mean ± SEM. $^{**}p < 0.01$, versus control; $^{\#}p < 0.05$ and $^{\#\#}p < 0.01$, versus model.

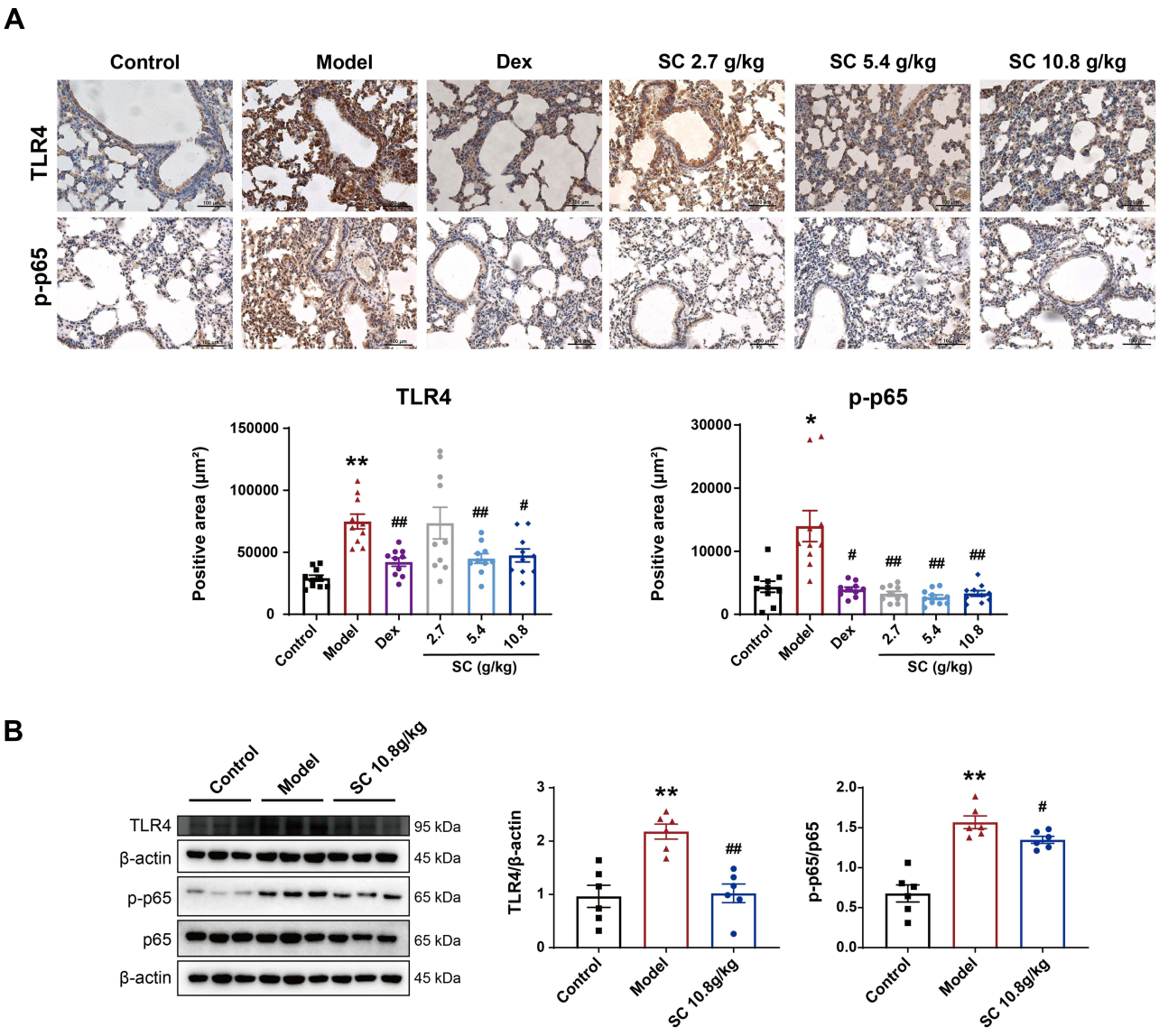

Figure 3 Effects of SC treatment on TLR4 and p-p65 expression in LPS-induced ALI mice. (**A**) Representative images of lung tissue immunostained with TLR4 and p-p65 and quantification of TLR4 and p-p65 positive area in lung tissues (n=10/group, Brown-Forsythe and Welch ANOVA tests for TLR4, Kruskal–Wallis test for p-p65). (**B**) Representative immunoblots and quantification of TLR4 and p-p65 in lung tissues (n=6/group, unpaired two-tailed *t*-test). β-actin was used as a loading control. Data are presented as the mean ± SEM. $^{*}p < 0.05$ and $^{**}p < 0.01$, versus control; $^{\#}p < 0.05$ and $^{\#\#}p < 0.01$, versus model.

SC Treatment Inhibited the Nuclear Translocation of NF-κB, AP-1, and IRF3 in LPS-Stimulated RAW264.7 Cells

After LPS stimulation, transcription factors, including NF-κB, AP-1, and IRF3, enter the nucleus from the cytoplasm and activate the transcription of pro-inflammatory mediator genes, thereby facilitating inflammatory responses.[24] As revealed by immunofluorescence, LPS exposure markedly triggered the nuclear translocation of AP-1 subunit c-Jun, NF-κB subunit p65, and IRF3, while SC treatment decreased the nuclear translocation of c-Jun, p65, and IRF3 in a concentration-dependent manner (Figure 6A). In line with that, the expression levels of p65, c-Jun, and IRF3 in the nuclear fraction of LPS-exposed RAW264.7 cells were significantly downregulated with SC treatment. Additionally, the expression of cytoplasmic proteins of p65, c-Jun, and IRF3 was not changed after SC treatment (Figure 6B). These findings implied the inhibitory effect of SC on nuclear translocation of NF-κB, AP-1, and IRF3.

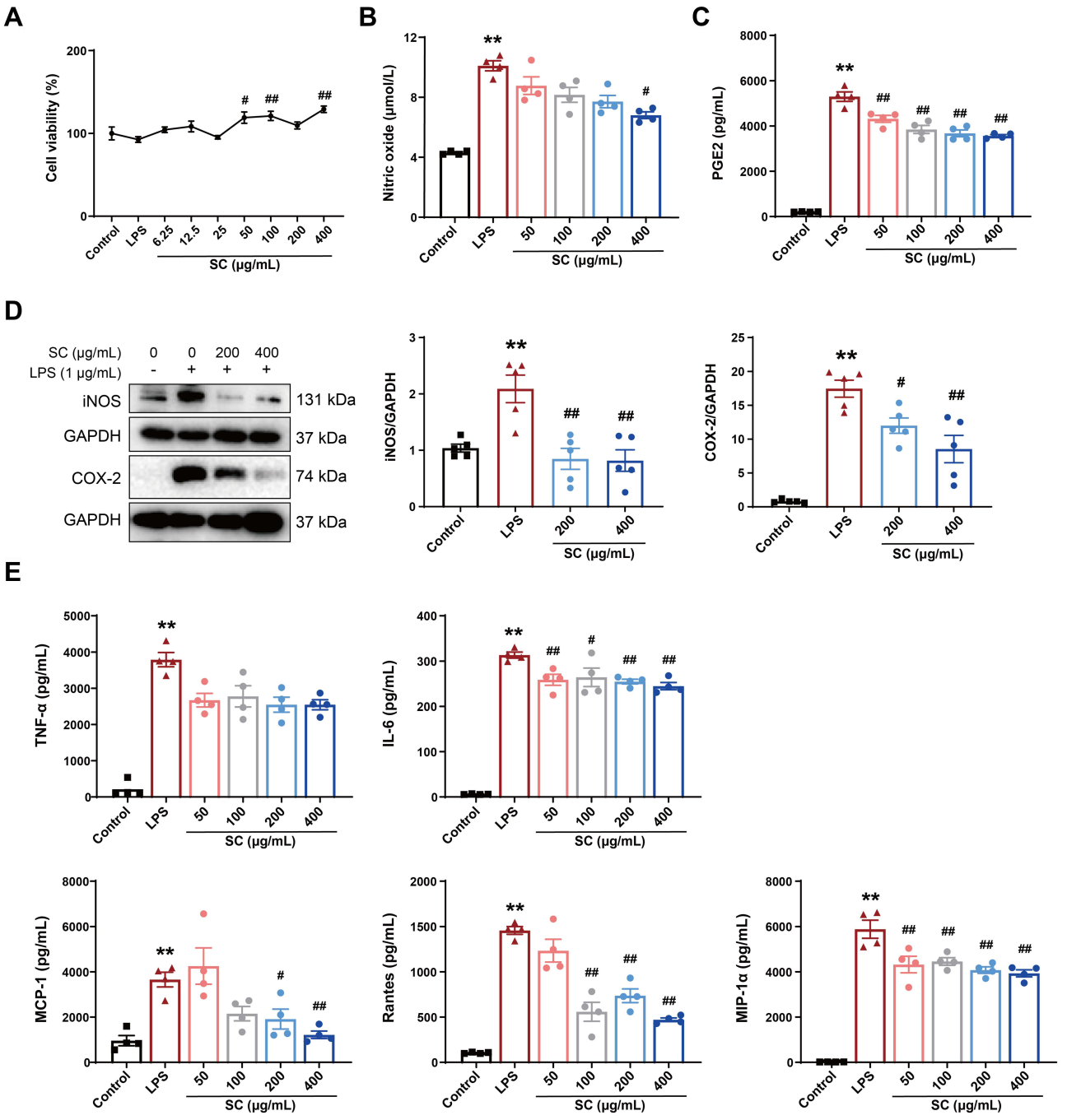

Figure 4 Effects of SC treatment on the production of pro-inflammatory mediators in LPS stimulated RAW264.7 cells. Cells were pretreated with SC at various concentration for 1 hour and then exposed to 1 μg/mL LPS for 24 hours. (**A**) Cell viability was determined by MTT assay (n=6/group, Kruskal–Wallis tests with Dunn's multiple comparisons as post hoc test). Levels of NO (**B**) and PGE2 (**C**) in culture media were measured by Griess assay and ELISA, respectively (n=4/group, Kruskal–Wallis test for NO, one-way ANOVA with Dunnett's post hoc test for PGE2). (**D**) Protein levels of iNOS and COX-2 in RAW264.7 macrophages were determined by Western blotting with GAPDH used as loading control (n=5/group, one-way ANOVA with Dunnett's post hoc test). (**E**) Levels of TNF-α, IL-6, MCP-1, Rantes and MIP-1α in the culture medium were determined by ELISA (n=4/group, Kruskal–Wallis test for TNF-α, one-way ANOVA with Dunnett's post hoc tests for IL-6, MCP-1, Rantes and MIP-1α). Data are presented as the mean ± SEM. $^{**}p < 0.01$, versus control; $^{\#}p < 0.05$ and $^{\#\#}p < 0.01$, versus LPS.

Discussion

ALI, a continuum of pulmonary changes arising from various lung injuries, is associated with poor prognosis and can even cause life-threatening respiratory failure in patients.[3] Current drug treatment options for ALI are not satisfactory because of their serious side effects and high cost. Traditional Tibetan medicine/formula may provide a good source to

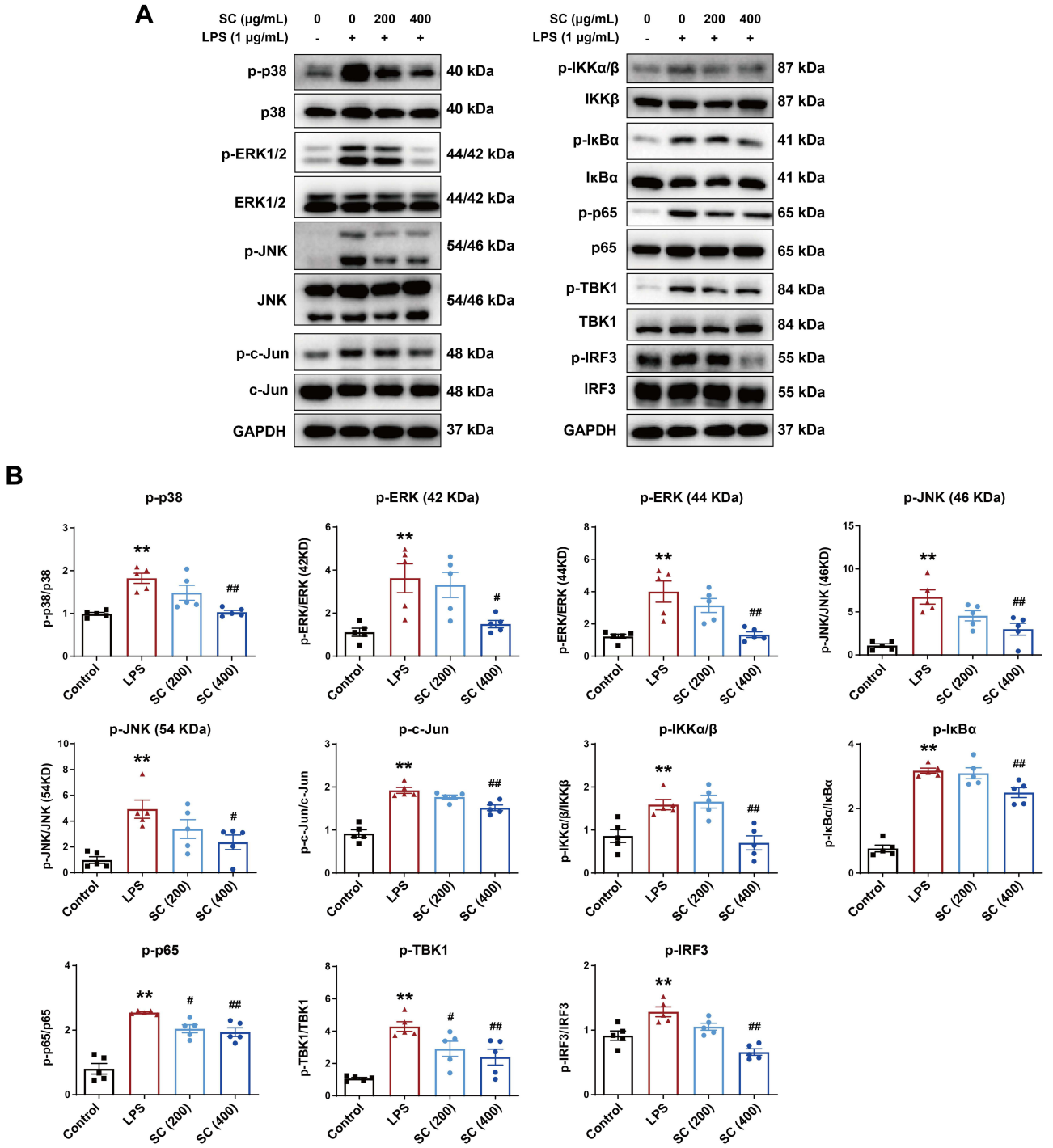

Figure 5 Effects of SC treatment on the TLR4 signaling pathway in LPS stimulated RAW264.7 cells. Cells were pretreated with SC at 200 μg/mL or 400 μg/mL for 1 hour and then incubated with 1 μg/mL LPS for 30 minutes. (**A**) Protein levels of the total and phosphorylated p38, JNK, ERK, c-Jun, IKK, IκBα, p65, TBK1 and IRF3 were detected by Western blotting with GAPDH used as loading control. (**B**) Bar graphs show the relative expression of indicated proteins (n=5/group, one-way ANOVA with Dunnett's post hoc test). Data are presented as the mean ± SEM. $^{**}p < 0.01$, versus control; $^{\#}p < 0.05$ and $^{\#\#}p < 0.01$, versus LPS.

develop safe and effective agents for the management of various diseases,[25] especially for respiratory diseases such as ALI.[26] In the present study, we found that SC, a classic Tibetan herbal formula for the treatment of acute and chronic respiratory diseases, ameliorated LPS-induced inflammatory responses in vivo and in vitro. It has been reported that several compounds identified in SC, including bergenin, chlorogenic acid, and monoammonium glycyrrhizinate, possess

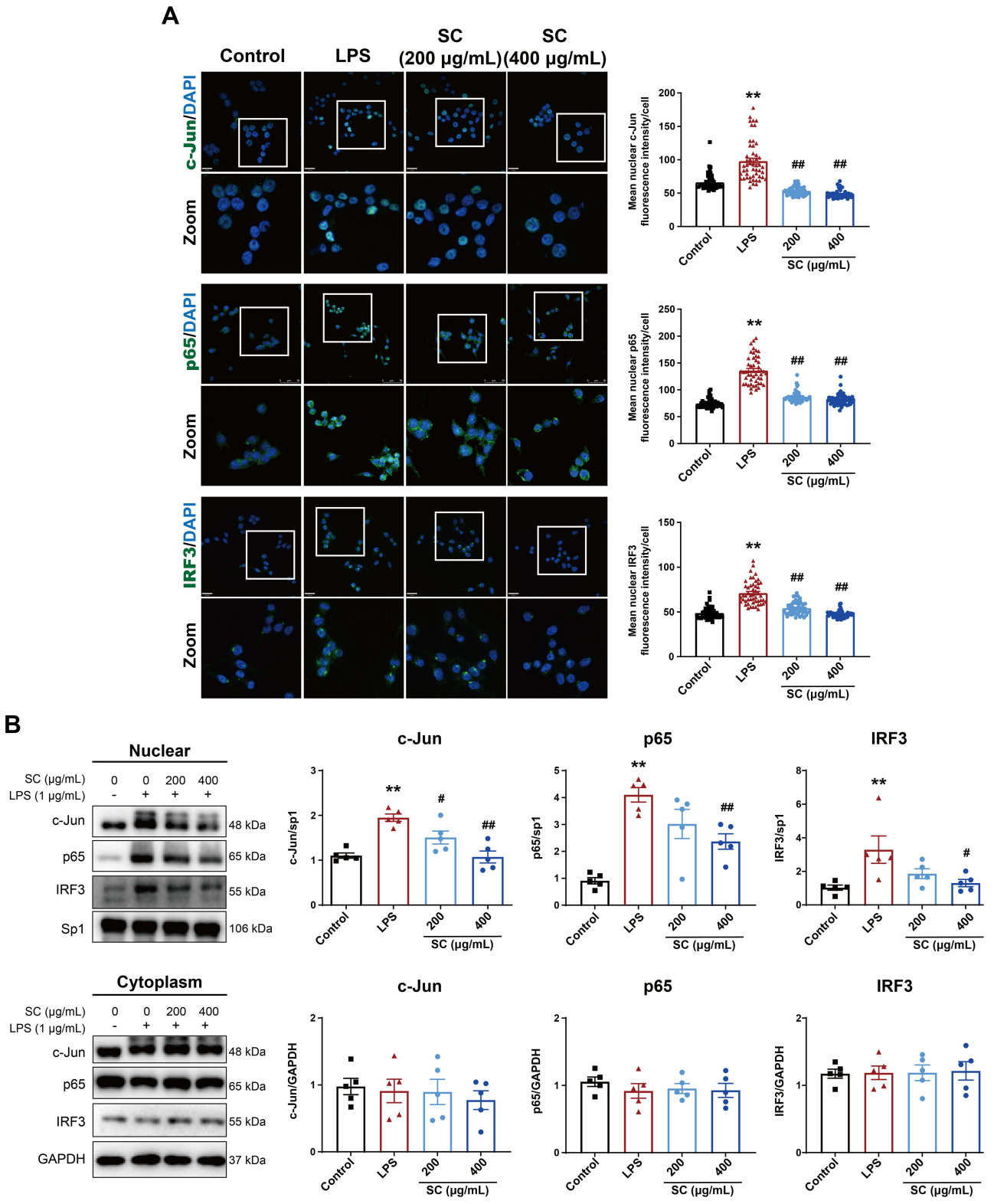

Figure 6 Effects of SC treatment on the nuclear translocation of NF-κB, AP-1, and IRF3 in LPS stimulated RAW264.7 cells. Cells were pretreated with 200 μg/mL or 400 μg/mL SC for 1 hour and then incubated with 1 μg/mL LPS for 30 minutes. (**A**) The cellular location of c-Jun, p65 and IRF3 was detected by immunofluorescence. Scale bars: 17 μM for c-Jun and IRF3, 50 μM for p65. Quantitative analysis was performed by ImageJ software (n = 50 cells per condition, Kruskal–Wallis test followed by Dunn's multiple comparisons test). (**B**) Protein levels of c-Jun, p65 and IRF3 in the nuclear and cytoplasm fractions of RAW264.7 macrophages were determined by Western blotting with Sp1/GAPDH used as loading controls. Bar graphs show the relative expression of indicated proteins (n=5/group, one-way ANOVA with Dunnett's post hoc test). Data are presented as the mean ± SEM. $^{**}p < 0.01$, versus control; $^{\#}p < 0.05$ and $^{\#\#}p < 0.01$, versus LPS.

potential anti-inflammatory activities.[27–29] We also found that these compounds could bind to TLR4, revealing that the anti-inflammatory effect of SC may be partially due to the presence of these bioactive compounds. Our further study will be conducted to identify the main active components responsible for the anti-inflammatory effect of SC.

Intra-alveolar macrophages play a critical part in releasing various inflammatory mediators that enhance the recruitment of defensive phagocytic cells, such as neutrophils, monocytes, and other immune effector cells, into the lung, particularly in response to acute and chronic pulmonary infections, leading to alveolar epithelial injury and the disruption of lung function.[30] Our work showed that there was a significant alleviation of the increased airway responsiveness in SC-treated rats with chronic bronchitis (data not shown), suggesting that SC has the potential to improve the lung function. With the use of the LPS-induced mouse model of ALI, we found that SC treatment inhibited the secretion of cytokines (TNF-α, IL-6, and IL-1β) and chemokines (MCP-1, MIP-1α, and RANTES) in BALF. We also observed that SC treatment inhibited alveolar immune cell infiltration, especially macrophages, as shown by HE and Wright stains. Moreover, we found that the administration of SC in mice with LPS exposure resulted in a significant reduction in CD68 levels, a surface marker expressed predominantly by macrophages,[31] which confirmed the ability of SC to inhibit macrophage activation upon LPS challenge. Hence, the anti-inflammatory action of SC may be related to its inhibitory effect on the activation of macrophages.

Stimulation of TLR4 signaling cascade by its ligands, such as LPS, is involved in the development and progression of ALI.[32] The TLR4 signaling can trigger the activation of two downstream signaling pathways, including MyD88-dependent and TRIF-dependent pathways. The activation of these two signaling pathways promotes the nuclear translocation of NF-κB, AP-1, and IRF3 and facilitates pro-inflammatory gene transcription, such as those coding TNF-α, IL-6, IL-1β, MCP-1, MIP-1α, and RANTES.[32] In the LPS-induced ALI mouse model, we found that SC could attenuate the recruitment of TLR4 and phosphorylation of NF-κB upon LPS exposure, indicating that SC has the potential to hinder the TLR4 signaling pathways. Thus, we investigated whether SC could prevent the subsequent LPS-mediated activation of the TLR4-related signaling pathways in cultured macrophages. In line with the in vivo study, SC treatment inhibited the LPS-induced release of pro-inflammatory inflammatory mediators, such as NO, PGE2, IL-6, MCP-1, MIP-1α, and RANTES in RAW264.7 macrophages. It has been reported that iNOS and COX-2 are the important enzymes generating NO and PGE2, respectively.[33] Our results also showed that SC treatment inhibited the expression of iNOS and COX-2 in LPS-stimulated macrophages, suggesting that SC treatment inhibits the production of NO and PGE2 by suppressing the activity of iNOS and COX-2, respectively. These results demonstrated that SC exerts a potent repressive effect on inflammatory responses in LPS-challenged macrophages. Meanwhile, our results showed that SC treatment inhibited the phosphorylation of NF-κB, AP-1, and IRF3. We also found that SC treatment hindered the nuclear translocation of these three transcription factors, indicating that SC could inhibit the TLR4 signaling pathways in LPS-exposed macrophages. Therefore, we further explored the upstream events of the activation of these three transcription factors. Studies have shown that the activation of NF-κB is mediated by the IKK complex with subsequent phosphorylation and degradation of IκB proteins.[34] In our present study, we found that the expression levels of phosphorylated IKKα/β, IκBα, and p65 were decreased after SC treatment in LPS-stimulated macrophages. Of note, the nuclear translocation of p65 was also suppressed by SC treatment, indicating that SC impedes the TLR4/IKKα/β/NF-κB signaling transduction. TLR4 activation by LPS also recruits MAPKs, including p38, ERK, and JNK, and promotes the nuclear translocation of AP-1.[35] We found that SC could inhibit the phosphorylation of p38, ERK, and JNK. It also reduced phosphorylated AP-1 subunit c-Jun and the nuclear localization of c-Jun, suggesting that SC inhibited the TLR4/MAPKs/c-Jun signaling pathway. Additionally, TBK1 is a serine/threonine-protein kinase phosphorylating IRF3, which dissociates from the adapter proteins, dimerizes, and then enters the nucleus.[36] Our results showed that SC treatment effectively suppressed the expression levels of phosphorylated TBK1 and IRF3 and its nuclear translocation, showing that SC also inhibited the TLR4/TBK1/IRF3 signaling pathway in LPS-stimulated macrophages.

Our study has some limitations. Firstly, the sample size of inflammatory mediator determination in vitro was small (n = 4). Because of the disruption in the distribution of ELISA kits caused by the COVID-19 pandemic, we could not repeat this experiment within the specified time period. Secondly, the effect of SC on lung function (e.g. airway resistance) in LPS-induced ALI mouse model should be evaluated. Thirdly, adoptive macrophage transfer studies should be designed to investigate the suppressive effect of inflammatory response by SC treatment. Thus, we will conduct these experiments in the future study to further verify the therapeutic role of SC in inflammatory pulmonary diseases.

Conclusions

Taken together, our present study showed that SC effectively inhibited the inflammatory responses in LPS-induced ALI mouse model/RAW264.7 macrophages. The underlying mechanism of this action might be associated with its inhibitory effect on the TLR4 signaling transduction, thereby suppressing the secretion of inflammatory mediators by immune cells, such as macrophages. These findings provide a pharmacological justification for the use of SC in the treatment of pulmonary inflammation for various respiratory diseases.

Abbreviations

SC, Sichen formula; ALI, acute lung injury; LPS, lipopolysaccharide; BALF, bronchoalveolar lavage fluid; ELISA, enzyme-linked immunosorbent assay; ARDS, acute respiratory distress syndrome; TLR, toll-like receptor; IκB, inhibitor of nuclear factor-κB; NF-κB, nuclear factor-κB; IKK, IκBα kinase; JNK, c-Jun N-terminal kinase; MAPK, mitogen-activated protein kinase; ERK, extracellular signal-regulated kinase; AP-1, activator protein 1; TBK, TANK-binding kinase; IRF, interferon regulatory factor; MTT, 3-[4,5-dimethylthiazol-2-yl]-2,5-diphenyl tetrazolium bromide; FBS, fetal bovine serum; DMEM, Dulbecco's Modified Eagle Medium; TNF-α, tumor necrosis factor-α; IL, interleukin; MIP-1α, macrophage inflammatory protein 1α; MCP-1, monocyte chemoattractant protein 1; RANTES, regulated upon activation normal T cell expressed and secreted factor; PGE2, prostaglandin E2; COX-2, cyclooxygenase-2; iNOS, inducible nitric oxide synthase; Ig, immunoglobulin; DAPI, 4′,6-diamidino-2-phenylindole; SEM, standard error of the mean.

Supplementary Material

All the original blots were provided in Supplement Material.

Ethics Approval

All the animal studies followed the National Institutes of Health Guide for the Care and Use of Laboratory Animals and approved by the Animal Care and Welfare Committee of Beijing University of Chinese Medicine [Certificate No. BUCM-4-2021031103-1048].

Acknowledgments

We thank Prof. Gan Luo for his work on molecular docking simulation.

Author Contributions

All authors made a significant contribution to the work reported, whether that is in the conception, study design, execution, acquisition of data, analysis and interpretation, or in all these areas; took part in drafting, revising or critically reviewing the article; gave final approval of the version to be published; have agreed on the journal to which the article has been submitted; and agree to be accountable for all aspects of the work.

Funding

This work was supported by the Key Science and Technology Research Projects of Tibet Autonomous Region of China (XZ201801-GA-16).

Disclosure

The authors report no conflicts of interest in this work.

References

1. Matthay MA, Zemans RL, Zimmerman GA, et al. Acute respiratory distress syndrome. *Nat Rev Dis Primers*. 2019;5(1):18. doi:10.1038/s41572-019-0069-0
2. Ashbaugh D, Bigelow DB, Petty T, Levine B. Acute respiratory distress in adults. *Lancet*. 1967;290(7511):319–323. doi:10.1016/S0140-6736(67)90168-7
3. Butt Y, Kurdowska A, Allen TC. Acute lung injury: a clinical and molecular review. *Arch Pathol Lab Med*. 2016;140(4):345–350. doi:10.5858/arpa.2015-0519-RA

4. Bellani G, Laffey JG, Pham T, et al. Epidemiology, patterns of care, and mortality for patients with acute respiratory distress syndrome in intensive care units in 50 countries. *JAMA*. 2016;315(8):788–800. doi:10.1001/jama.2016.0291
5. Sevransky JE, Levy MM, Marini JJ. Mechanical ventilation in sepsis-induced acute lung injury/acute respiratory distress syndrome: an evidence-based review. *Crit Care Med*. 2004;32(11 Suppl):S548–53. doi:10.1097/01.CCM.0000145947.19077.25
6. Villar J, Ferrando C, Martínez D, et al. Dexamethasone treatment for the acute respiratory distress syndrome: a multicentre, randomised controlled trial. *Lancet Respir Med*. 2020;8(3):267–276. doi:10.1016/S2213-2600(19)30417-5
7. Levy BD, Serhan CN. Resolution of acute inflammation in the lung. *Annu Rev Physiol*. 2014;76:467–492. doi:10.1146/annurev-physiol-021113-170408
8. Lee JW, Chun W, Lee HJ, et al. The role of macrophages in the development of acute and chronic inflammatory lung diseases. *Cells*. 2021;10(4):897. doi:10.3390/cells10040897
9. Lawrence T. The nuclear factor NF-kappaB pathway in inflammation. *Cold Spring Harb Perspect Biol*. 2009;1(6):a001651. doi:10.1101/cshperspect.a001651
10. Carter AB, Monick MM, Hunninghake GW. Both Erk and p38 kinases are necessary for cytokine gene transcription. *Am J Respir Cell Mol Biol*. 1999;20(4):751–758. doi:10.1165/ajrcmb.20.4.3420
11. Kumar V. Pulmonary innate immune response determines the outcome of inflammation during pneumonia and sepsis-associated acute lung injury. *Front Immunol*. 2020;11:1722. doi:10.3389/fimmu.2020.01722
12. Ge-Sang CR, Yu RY. Acute toxicity study of Tibetan medicine Sichen formula. *J Med Pharm Chins Minor*. 2014;20(10):48. doi:10.16041/j.cnki.cn15-1175.2014.10.029 [in Chinese]
13. Qin LY, Cai MR, Yao Y, et al. HPLC fingerprints of Tibetan medicine Sichen Zhike granules. *Central South Pharm*. 2021;19(03):507–512. doi:10.7539/j.issn.1672-2981.2021.03.023 [in Chinese]
14. Wang JL, Zhou HY, Dun, Z, Pan, D. Pharmacodynamic research on antitussive effect of Tibet medicine Si Chen Zhi Ke Granule. *Chin J Tradit Chin Med Pharm*. 2007;22(12):895–898. [in Chinese]
15. Seeliger D, de Groot BL. Ligand docking and binding site analysis with PyMOL and Autodock/Vina. *J Comput Aided Mol Des*. 2010;24(5):417–422. doi:10.1007/s10822-010-9352-6
16. Mirzapoiazova T, Kolosova IA, Moreno L, Sammani S, Garcia JG, Verin AD. Suppression of endotoxin-induced inflammation by taxol. *Eur Respir J*. 2007;30(3):429–435. doi:10.1183/09031936.00154206
17. Tsai CL, Lin YC, Wang HM, Chou TC. Baicalein, an active component of Scutellaria baicalensis, protects against lipopolysaccharide-induced acute lung injury in rats. *J Ethnopharmacol*. 2014;153(1):197–206. doi:10.1016/j.jep.2014.02.010
18. Luo G, Cheng BC, Zhao H, et al. Schisandra Chinensis Lignans suppresses the production of inflammatory mediators regulated by NF-κB, AP-1, and IRF3 in Lipopolysaccharide-stimulated RAW264.7 cells. *Molecules*. 2018;23(12):3319. doi:10.3390/molecules23123319
19. Zhang Y, Chi-Yan Cheng B, Xie R, Xu B, Gao XY, Luo G. Re-Du-Ning inhalation solution exerts suppressive effect on the secretion of inflammatory mediators via inhibiting IKKα/β/IκBα/NF-κB, MAPKs/AP-1, and TBK1/IRF3 signaling pathways in lipopolysaccharide stimulated RAW 264.7 macrophages. *RSC Adv*. 2019;9(16):8912–8925. doi:10.1039/C9RA00060G
20. Malik K, Ahmad M, Zhang G, et al. Traditional plant based medicines used to treat musculoskeletal disorders in Northern Pakistan. *Eur J Intergr Med*. 2018;19:17–64. doi:10.1016/j.eujim.2018.02.003
21. Yue Y, Li Q, Fu Y, Chang J. Stability of chlorogenic acid from artemisiae scopariae herba enhanced by natural deep eutectic solvents as green and biodegradable extraction media. *ACS Omega*. 2021;6(50):34857–34865. doi:10.1021/acsomega.1c05541
22. Asl MN, Hosseinzadeh H. Review of pharmacological effects of Glycyrrhiza sp. and its bioactive compounds. *Phytother Res*. 2008;22(6):709–724. doi:10.1002/ptr.2362
23. Chen H, Jiang Z. The essential adaptors of innate immune signaling. *Protein Cell*. 2013;4(1):27–39. doi:10.1007/s13238-012-2063-0
24. Hu R, Xu H, Jiang H, Zhang Y, Sun Y. The role of TLR4 in the pathogenesis of indirect acute lung injury. *Front Biosci*. 2013;18(4):1244–1255. doi:10.2741/4176
25. Yan LS, Cheng BC, Zhang SF, et al. Tibetan medicine for diabetes mellitus: overview of pharmacological perspectives. *Front Pharmacol*. 2021;12:748500. doi:10.3389/fphar.2021.748500
26. Fu K, Xu M, Zhou Y, et al. The Status quo and way forwards on the development of Tibetan medicine and the pharmacological research of Tibetan materia Medica. *Pharmacol Res*. 2020;155:104688. doi:10.1016/j.phrs.2020.104688
27. Yang S, Yu Z, Wang L, et al. The natural product bergenin ameliorates lipopolysaccharide-induced acute lung injury by inhibiting NF-kappaB activation. *J Ethnopharmacol*. 2017;200:147–155. doi:10.1016/j.jep.2017.02.013
28. Zhang X, Huang H, Yang T, et al. Chlorogenic acid protects mice against lipopolysaccharide-induced acute lung injury. *Injury*. 2010;41(7):746–752. doi:10.1016/j.injury.2010.02.029
29. Shi JR, Mao LG, Jiang RA, Qian Y, Tang HF, Chen JQ. Monoammonium glycyrrhizinate inhibited the inflammation of LPS-induced acute lung injury in mice. *Int Immunopharmacol*. 2010;10(10):1235–1241. doi:10.1016/j.intimp.2010.07.004
30. Maus U, von Grote K, Kuziel WA, et al. The role of CC chemokine receptor 2 in alveolar monocyte and neutrophil immigration in intact mice. *Am J Respir Crit Care Med*. 2002;166(3):268–273. doi:10.1164/rccm.2112012
31. Holness CL, Simmons DL. Molecular cloning of CD68, a human macrophage marker related to lysosomal glycoproteins. *Blood*. 1993;81(6):1607–1613. doi:10.1182/blood.V81.6.1607.1607
32. Jeyaseelan S, Chu HW, Young SK, Freeman MW, Worthen GS. Distinct roles of pattern recognition receptors CD14 and Toll-like receptor 4 in acute lung injury. *Infect Immun*. 2005;73(3):1754–1763. doi:10.1128/IAI.73.3.1754-1763.2005
33. Murakami A, Ohigashi H. Targeting NOX, INOS and COX-2 in inflammatory cells: chemoprevention using food phytochemicals. *Int J Cancer*. 2007;121(11):2357–2363. doi:10.1002/ijc.23161
34. Oeckinghaus A, Hayden MS, Ghosh S. Crosstalk in NF-κB signaling pathways. *Nat Immunol*. 2011;12(8):695–708. doi:10.1038/ni.2065
35. Yang H, Young DW, Gusovsky F, Chow JC. Cellular events mediated by lipopolysaccharide-stimulated toll-like receptor 4. MD-2 is required for activation of mitogen-activated protein kinases and Elk-1. *J Biol Chem*. 2000;275(27):20861–20866. doi:10.1074/jbc.M002896200
36. Perry AK, Chow EK, Goodnough JB, Yeh WC, Cheng G. Differential requirement for TANK-binding kinase-1 in type I interferon responses to toll-like receptor activation and viral infection. *J Exp Med*. 2004;199(12):1651–1658. doi:10.1084/jem.20040528